Journal of Materials and Applications 2024;13(1):11-20
https://doi.org/10.32732/jma.2024.13.1.11

# Evolution of Microstructure During Stress Relieving Heat Treatment of 1S Aluminium

Gargi Choudhuri

*Quality Assurance Division, Bhabha Atomic Research Centre, Mumbai, 400085, India*
*E-mail: gargi@barc.gov.in*

Received: 31 January 2024; Accepted: 5 March 2024; Available online: 30 May 2024

**Abstract:** Aluminium and its alloys are extensively used in nuclear research reactors due to its low neutron absorption coefficient, good heat transfer properties, excellent corrosion and oxidation resistance in air and water environment combined with desirable mechanical properties along with considerable radiation stability. The thin walled tubes are normally manufactured through port hole die extrusion route and used in 'O' tempered condition. The thin tubes in 'O' tempered condition are undergone canning operation which may alter the microstructural features to some extent which may affect mechanical properties. The paper describes the extent to which microstructural and subsequently mechanical properties are altered due to the simulated canning process and further requirements of stress relieving heat treatment to restore the microstructural features and mechanical properties. The following studies are carried out with 1S aluminum tube in 'O' tempered state, simulated canning condition and stress relieved at different temperature, - hardness measurement, X ray line profile analysis for dislocation density measurement, tensile properties measurement using ring tensile testing, electron back scattered diffraction (EBSD) analysis for recrystallization fraction determination and changes in texture components. It is found that the canning operation changes dislocation density, micro-strain, coherent domain size which are well reflected in hardness and ring tensile testing. Subsequent stress relieving at 350°C for 2 hrs. leads to improvement of mechanical properties appreciably.
**Keywords***:* 1S Al; Port hole die extrusion; X ray line profile analysis; Stress releiving heat treatment.

## 1. Introduction

99.5 % pure 1S Aluminum is widely being used as clad tube for research reactors [1-2] due to its low neutron absorption coefficient, good corrosion and oxidation resistance in water environment combined with good mechanical properties. The thin-walled aluminum tubes having grade 1050/1060/1070 are normally manufactured through hot extrusion route (either Seamless or Port-Hole Technique) [3-18] and used in Temper Condition 'O' of ASTM B-221 standard specification. The extruded tubes should have sufficient ductility and strength to further undergo canning operation. During the canning operation [19], the tube is subjected to further cold drawn process using a moving mandrel. Hence subsequent stress relieving may be helpful to restore the ductility. To understand the extent to which changes in mechanical properties occurs during canning and subsequent stress relieving process, the following studies were carried out with 1S aluminium tube cold drawn under simulated condition.

1) Hardness measurement
2) X ray line profile analysis for dislocation density measurement [20-22].
3) Tensile properties measurement, using ring tensile testing.
4) Electron back scattered diffraction (EBSD) analysis for recrystallization fraction determination and changes in texture components.

Dislocation density (ρ) is one of the important material characteristics which influences in-reactor performance and out of pile properties of clad, pressure tube and other structural materials. There are two basic techniques for measurement of dislocation density from X-ray line profile analysis [20]: (i) Fourier space technique which involves Fourier analysis, (ii) real space techniques in which integral breadth analysis, or FWHM are the most popular. The correction for instrumental broadening is the most important steps in the estimation of material properties from line profile analysis.

Hardness measurement is the easiest and qualitative method for identifying the extent of softening during thermal treatment due to recovery and recrystallization. Various method using EBSD analysis provide more quantitative estimation of the degree of recrystallization. But each method has certain shortfall.

The purpose of this work is to find the extent stress relieving required to restore the microstructural and mechanical behaviour of canned 1S Aluminum tube to the desired extent.

## 2. Experimental procedure

1S Al tubes were taken in as received condition which is port hole die extruded and in tempered condition. In order to simulate the cladding operation, as received clad tubes were cold drawn with same die which is used during cladding process and with the plug having the same diameter as that of fuel. Hence the percentage reduction in area of the drawn tube is same as that of clad tube after actual canning operation (nearly 11%). The canned tubes were then stress relieved at five different temperatures for 2 hrs., viz. 180°C, 200°C, 250°C, 300°C, 350°C and 400°C respectively.

Metallographic sample preparation was carried out in all the samples. Samples were polished up to 1μm diamond finish followed by three stage electro polishing to ensure complete removal of deformed layer. Micro-hardness measurement were carried out in radial-circumferential plane using 100 gm load in Vicker's scale.

Dislocation density measurement were carried out on the as received tube (before canned), canned tube and canned tube subjected with two stress relieving treatment. viz.(i) 250°C/3 hrs. & (ii) 350°C/3 hrs. The specimen after different stress relieving conditions, were ground flat, polished mechanically and then electro chemically. The sample was then irradiated using Phillips expert pro machine with CuKα radiation falling on this surface. Scan step size was 0.02° and scan rate 0.5°per min. The peak broadening were measured for respective peaks after fitting Gaussian curve at different Bragg angles for all the conditions. The broadening of X ray peak occurs basically due to microstructural broadening (presence of dislocations, lattice stain, stacking faults) and size effects apart from instrumental broadening. When the sample is free from microstructural broadening due to dislocations, lattice stain etc. (fully annealed condition), FWHM due to instrumental broadening can be found from the Gaussian plot of the peak subtracting the background. This width (b) is a function of Bragg's diffraction angle(θ) [21].

$$(b)^2 = U\tan^2\theta + V\tan\theta + W \quad (1)$$

Fully annealed (400°C-2 hrs.) aluminum 1S tube having hardness HV-27, has been used for calculation of instrumental broadening. The raw data obtained for the four peaks of fully annealed sample is given in table 1. Using high intensities peaks, second order polynomial equation was fitted with Y axis as (b)^2 and X axis as tanθ. Equation (1) was used for calculating instrumental broadening (b) at any given angle θ. The high degree of fit (Fig.1) ensures correct correction due to instrumental effects.

Table1. X-ray peak data for 1S Aluminium in fully annealed condition

| Peak (2 θ) | tanθ | Max. Intensity | FWHM |
|---|---|---|---|
| **38.46** | 0.34882 | 1810 | **0.17652** |
| **44.72** | 0.41135 | 1798 | **0.1877** |
| **65.11** | 0.63842 | 122.8 | **0.28** |
| **78.25** | **0.8134** | **228** | **0.34125** |

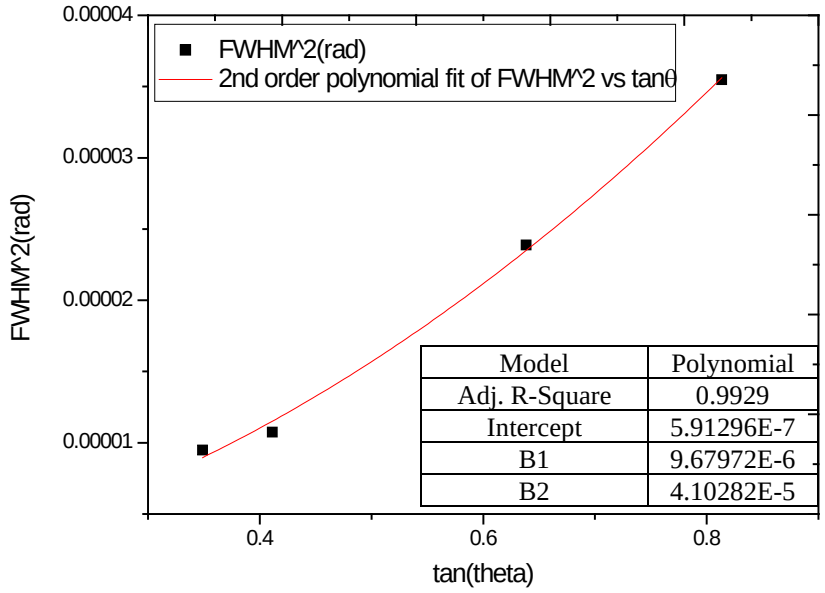


Fig.1. Second order polynomial fit for instrumental broadening in fully annealed 1S Al

The peak broadening (β) due to dislocation, micro strain, coherent domain at any angle for as extruded, canned and stress relieved material is found out after subtracting the instrumental broadening from total broadening of the respective peaks. To further separate the effect of broadening of X-ray line due to coherent domain D and micro-strain ε, following equation is used

$$\left(\frac{\beta \cos\theta}{\lambda}\right) = \left(\frac{1}{D}\right) + \left(\frac{4\varepsilon \sin\theta}{\lambda}\right) \quad (2)$$

where β=instrumental corrected broadening in radians, θ=Bragg's diffraction angle, D=Coherent domain size ($A^0$ ), ε=micro strain, λ= wave length ($A^0$) of X ray.

Linear equation was fitted between $\frac{\beta cos\theta}{\lambda}$vs. $\frac{sin\theta}{\lambda}$ . From the plot D and ε were calculated using the following equations, Intercept $= \frac{1}{D}$, slope=$4\varepsilon$. Finally dislocation density was calculated from coherent domain D & micro-strain ε using the following equations.

$$\boldsymbol{\rho_D = 3\eta/D^2} \quad (3)$$

where η=1

$$\boldsymbol{\rho_\epsilon = \varepsilon^2}/b^2 \quad (4)$$

where b is the burger vector $b = \frac{a_0}{3}[110]$, $a_0$ = 0.41 nm for Al

Dislocation density,

$$\rho = (\rho_D . \rho_\varepsilon)\text{^}0.5 \quad (5)$$

To know the mechanical properties, ring tensile testing of as-received, canned and in all the stress relieved samples were carried out. The ring tensile testing was carried out at room temperature using a screw-driven universal tensile testing machine at a cross-head speed of 0.5 mm/min. Typical ring tested specimen is shown in Figure 2a. Fig.2b shows the ring tensile testing sample after completion of the test. Gauge length of the ring specimens was estimated using the stamping method. Large variation was observed in the specimen to specimen gauge length estimation and hence the maximum observed gauge length of 7 mm was used for the analysis of all ring tensile tests irrespective of the specimen lot in the present study.

Fig. 2a Typical 3 mm wide ring tensile testing sample

Fig. 2b Typical ring tested sample

For EBSD analysis, Camscan 3200L scanning electron microscope equipped with a Nordlys attachment and the Oxford instruments HKL technology CHANNEL 5 software package has been used. Low angle boundaries (LABs) were plotted at misorientation angles in the range of 2-10°, and high angle boundaries (HABs) were plotted when misorientation angle exceeds 10° [23]. The average misorientation angle inside a grain, bounded by HABs has been determined. EBSD can be used for quantifying extent of recrystallization[24]. To calculate the recrystallized fraction, two methods are normally adopted. In the first method, a grain is termed as recrystallized grain, if the average misorientation angle inside it is less than 2° or no sub-grains. If the grain consists of sub-

grains bounded by LABs and if the average misorientation angle inside the sub-grains is less than 2°, these grains is classified as polygonized grains with substructure. All other grains are termed as deformed grains, i.e. average internal misorientation angle within a grain is greater than critical angle. An error in quantifying the recrystallization fraction may be introduced due to the presence of very small fraction of grains having misorientation angle <10°. Hence another technique can also used where the ratio of HABs to the total-boundary length are measured [25].

To detect the changes in texture component during canning process and subsequent annealing, orientation mapping as well as IPF-Z has been plotted for as received as well as canned tube to depict the change in intensity of texture.

## 3. Results and Discussion

Hardness plot of port hole die extruded, canned and subsequently stress relieved material is given in Fig.3. As received port hole die extruded samples have average hardness around HV 37. After canning operation average hardness increases to HV 41. With thermal treatment at 200°C for 2 hrs, no gross change in hardness occurs, But 250°C 2 hrs thermal treatment reduces hardness level to HV 38.5. Annealing at 300°C for 2 hrs lead to appreciable change in hardness (HV31). Further annealing at 350°C, hardness of the tube reduces to HV29. 400°C, 2 hrs thermal treatment lead to further reduction of hardness to HV27. The hardness plot with temperature clearly shows that there is an appreciable change in hardness when annealing temperature increases beyond 250°C, where T/Tm is 0.56. The common hardness temperature relationship can be written as; $H = Aexp(-BT)$ [26]

where H is hardness and T temperature in K. The constant, A, is found by extrapolation and is named as "intrinsic hardness" of the material, i.e. the hardness value at T=0 K and the constant B is the softening coefficient of hardness. The change in the value of A and B indicates change in the mechanism of softening. In the table 2, the values of A and B for the two temperature regions are given. It shows definite change in softening coefficient and intrinsic hardness value which indicates a change in mechanism.

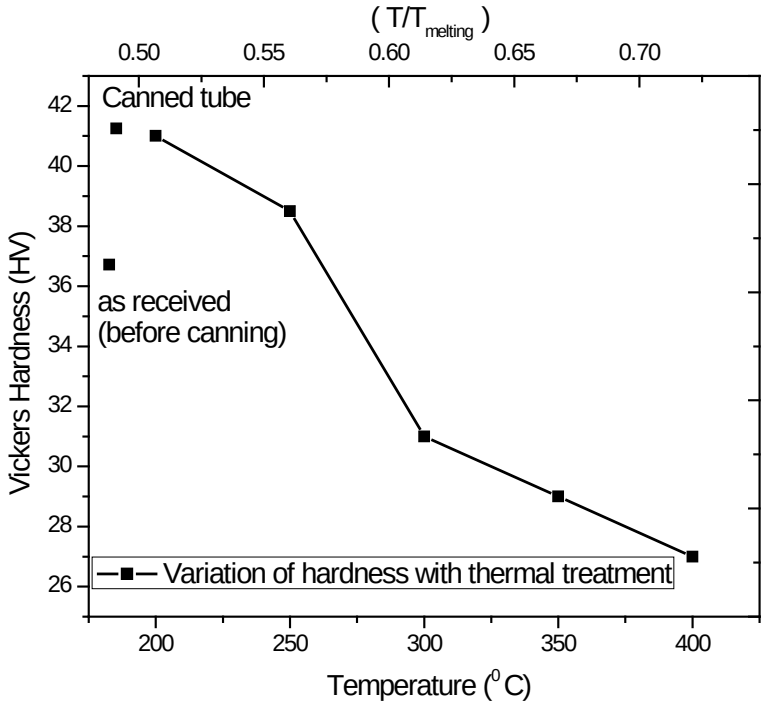


Fig. 3. Variation of hardness with temperature of the stress relieving treatment

Table 2. Intrinsic hardness and softening coefficient of 1S Al

| Temperature | A | B |
|---|---|---|
| 200-250°C | 74.34675 | 0.00126 |
| 300-400°C | 68.46893 | 0.00138 |

Results of LPA analysis are given in table 3 and the trend in dislocation density and micro-strain with canning and subsequent stress relieving treatment are given in Fig.4 a, b, c.

Table 3. Results of line profile analysis using integral breadth technique.

| Sample description | Dislocation density by XRD (Nos./m$^{2)}$ | Coherent domain size(A$^0$) | Micro-strain |
|---|---|---|---|
| As received | 2.6800E12 | 254.966 | 0.000114 |
| Canned | 2.2074E14 | 107.24 | 0.000395 |
| 250C-2 hrs | 1.0650E13 | 151.98 | 0.000270 |
| 350-2hrs | 5.0970E12 | 358.944 | 0.000097 |

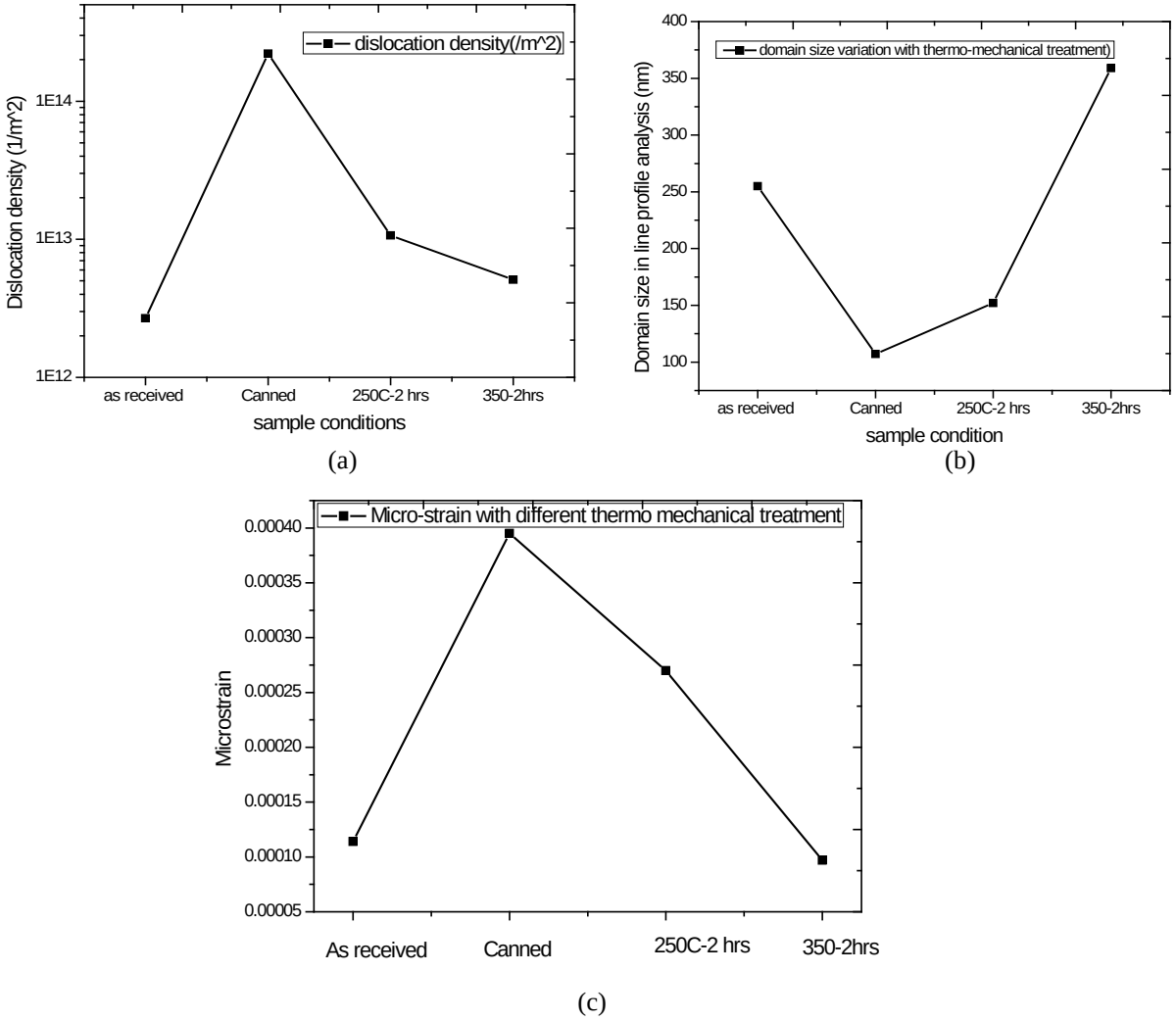


Fig. 4. Graphical representation of variation of (a) dislocation density, (b) coherent domain size and (c) micro-strain with different thermo mechanical treated samples of 1S Aluminum tube.

From the graphical representation, it is clearly visible that the canning operation appreciably changes the micro-structural parameters of 1S Al tube. After canning operation, dislocation density increases two order i.e. nearly 100 times from 2.6800E12 to 2.2074E14 nos./m^2 along with micro-strain. This operation also causes reduction of the coherent domain size. Subsequently 250ºC 2 hrs. stress relieving heat treatment causes one order reduction of dislocation density as well as decrease in micro-strain although hardness does not reduce significantly. Size of the coherent domain size increases. After 350ºC 2 hrs. stress relieving, dislocation density and micro-strain reduce significantly along with hardness. Size of the coherent domain size increases to 359 Å.

Fig.5a and Fig.5b depict the mis-orientation angle distribution of boundaries in as-received and after canning operation of thin walled Al tube. From the figures it is clearly seen that canning operation increases the low angle grain boundary fraction from 30% to 45%, considering high angle grain boundaries has greater than 10º misorientation and 2-10º has been considered as low angle grain boundary.

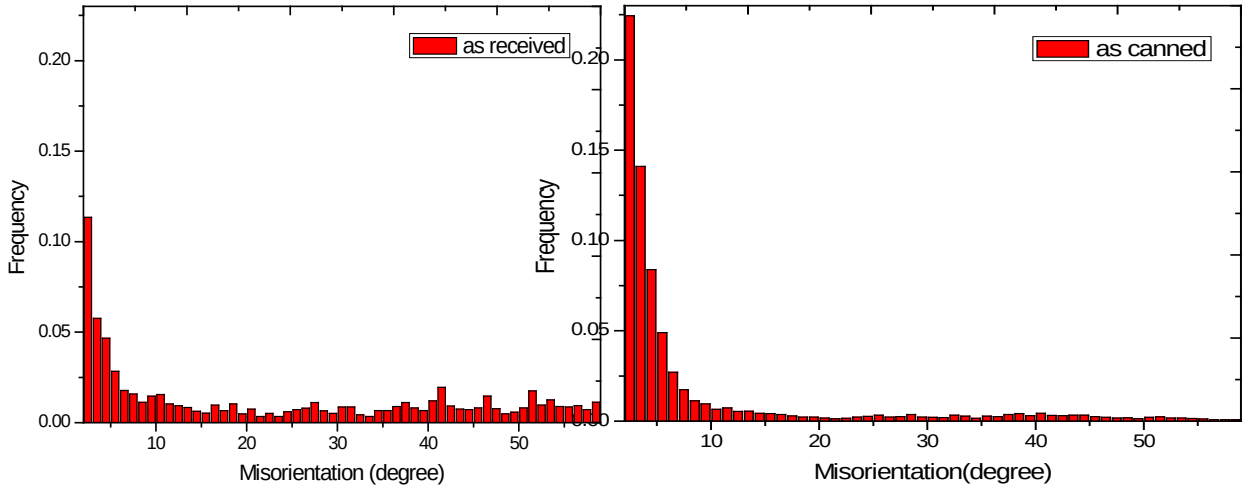


(a) (b)

Fig. 5. Misorientation angle distribution of grain boundaries in degree for (a) as received tube showing 30% low angle grain-boundary fraction (2-10°), (b) canned tube showing 45% low angle grain-boundary fraction (2-10°) indicates that the canning operation increases low angle grain boundary fraction.

Using the first method (although this method of finding recrystallization has certain drawbacks) to qualitatively compare the extent of recrystallization in both the samples before and after canning, it is found that in as-received material majority of grains are recrystallized grain (around 72.8%), 25.3% is of deformed grain and around 2% has substructure, i.e. polygonized grain in the microstructure (according to criteria given). Canning operation creates substructure (5.3%) as well as significant amount of deformed grains (91.6%) in the microstructure consuming recrystallized grains (table 4).

Table 4. Estimation of recrystallization fraction in as received and canned sample

| **% of recrystallized, sub-structure and deformed grains** | **$\Theta_{LAB}^{min.}(2^o) \leq \Theta \geq \Theta_{LAB}^{max.}(10^o)$** | |
|---|---|---|
| | **As Received** | **As Canned** |
| **Recrystallized** | 72.8 | 3.15 |
| **Sub Structure** | 1.96 | 5.27 |
| **Deformed grains** | 25.3 | 91.6 |

The orientation maps of as received tube and canned tube in z direction are given in Fig.6a and 6b. Major texture component is [100] and with [111] minor component in as received one. This 100 texture is the annealing texture in Aluminium, whereas after canning operation reduction in 100 texture components occurs which is also depicted in inverse pole figure in Z direction, IPF (z) representation (Fig.6c and 6d). All these results clearly indicates that canning operation changes the microstructural features, like dislocation density, coherent domain size, micro-strain, micro-texture and generates polygonized grains i.e. substructure and deformed grains consuming strain-free recrystallized grains.

The results of the ring tension tests are graphically depicted in Fig. 7 a, b, c, d which includes average tensile properties, viz. yield strength (YS), ultimate tensile strength (UTS), uniform elongation (UE) and total elongation (TE) for all the specimens types. Typical engineering stress-strain plots obtained for specimens from different lots is given in Fig. 8 [27].

As received sample has average Y.S 46.5 MPA. After canning operation Y.S increased to 69.2 Mpa. For 1 S aluminum, this increase in Y.S is significant. Whereas increase of UTS after canning operation occurs to a lesser extent (69.4 MPa to 81.5 MPa). But decrease in uniform elongation as well as total elongation after canning operation is significant. 250°C 2 hrs heat treatment do not change the Y.S and UTS value significantly, but percentage total elongation increases. As Y.S and UTS do not change, hence uniform elongation also does not show any changes. 350°C 2 hrs. stress relieving significantly improves the uniform as well as total elongation. Scatter in data point is significantly reduced in total elongation after 350°C 2 hrs stress relieving operation.

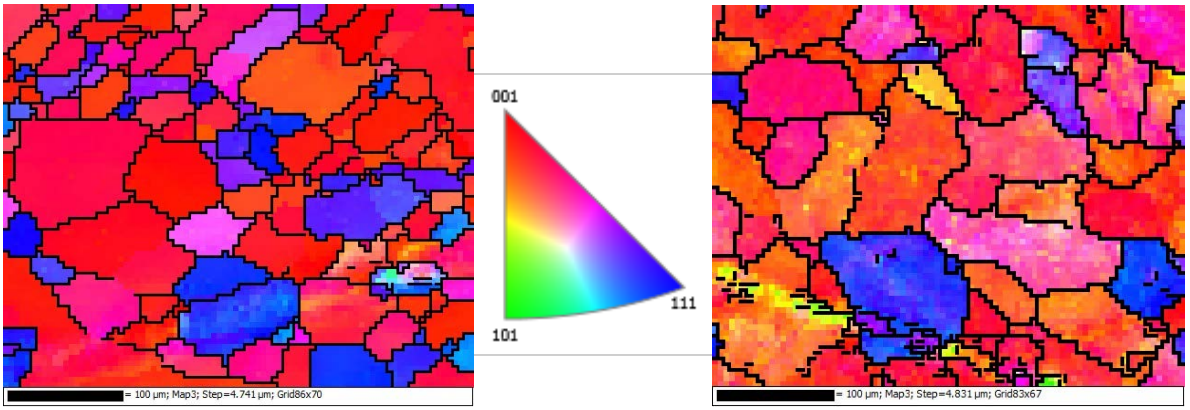


(a) Orientation map of IPF-Z of as-received 1S Aluminium.

(b) Orientation map of IPF-Z of 1S Aluminium after canning operation.

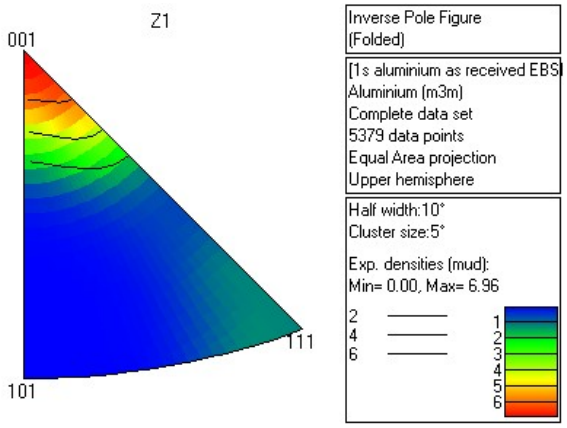


(c) Inverse pole figure (IPF-Z) of as-received 1S Aluminium which shows strong 100 texture .

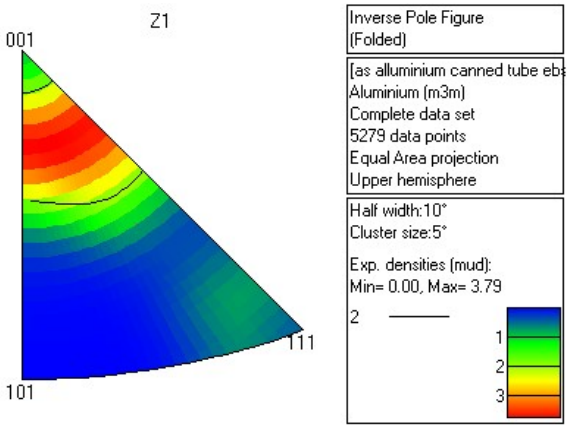


(d) Inverse pole figure (IPF-Z) of canned 1S Aluminium which shows reduction of annealing texture.

Fig. 6. Orientation maps (a, b), Inverse pole figure (c, d) representation (IPF-Z) of as received and canned one.

## 4. Conclusions

1) Hardness of port hole die extruded as received 1S Aluminum material increases significantly after canning operation (Avg. HV 41). With thermal treatment at 200°C for 2 hrs, no gross change in hardness occurs, But 250°C 2 hrs thermal treatment reduces hardness level to HV 38.5. Annealing at 300°C for 2 hrs leads to appreciable change in hardness (HV31). Further annealing at 350°C, hardness of the tube reduces to HV29.

2) Line profile analysis has been carried out for measurement of dislocation density, coherent domain size and micro strain in as received, canned, and stress relieved at two different temperatures (250ºC and 350ºC).

3) Starting tube has dislocation density $2.68 \times 10^{12}$ /m^2. Canned tube shows approximately two order increase in dislocation density, $2.2 \times 10^{14}$ /m^2. 250°C-2 hrs stress relieving leads to reduction of dislocation density of one order ($1.1 \times 10^{13}$ /m^2) but 350ºC -2 hrs. heat treatment leads to significant reduction of dislocation density ($5.1 \times 10^{12}$ /m^2). There is also progressively increase in coherent domain size and decrease in micro-strain with stress relieving.

4) Ring tensile testing results show that cold work during canning leads to increase in yield and ultimate tensile strength of as-canned clad material accompanied by the reduction in ductility as compared to that of the port hole die extruded clad tube. Heat treatment of canned material for 200ºC, 250ºC for 2 hours leads to recovery in material in terms of marginal decrease in average ultimate tensile strength and increase in ductility as compared to that of as-canned material, whereas 350ºC 2 hrs. stress relieving leads to appreciable improvement in ductility without compromising Y.S and UTS.

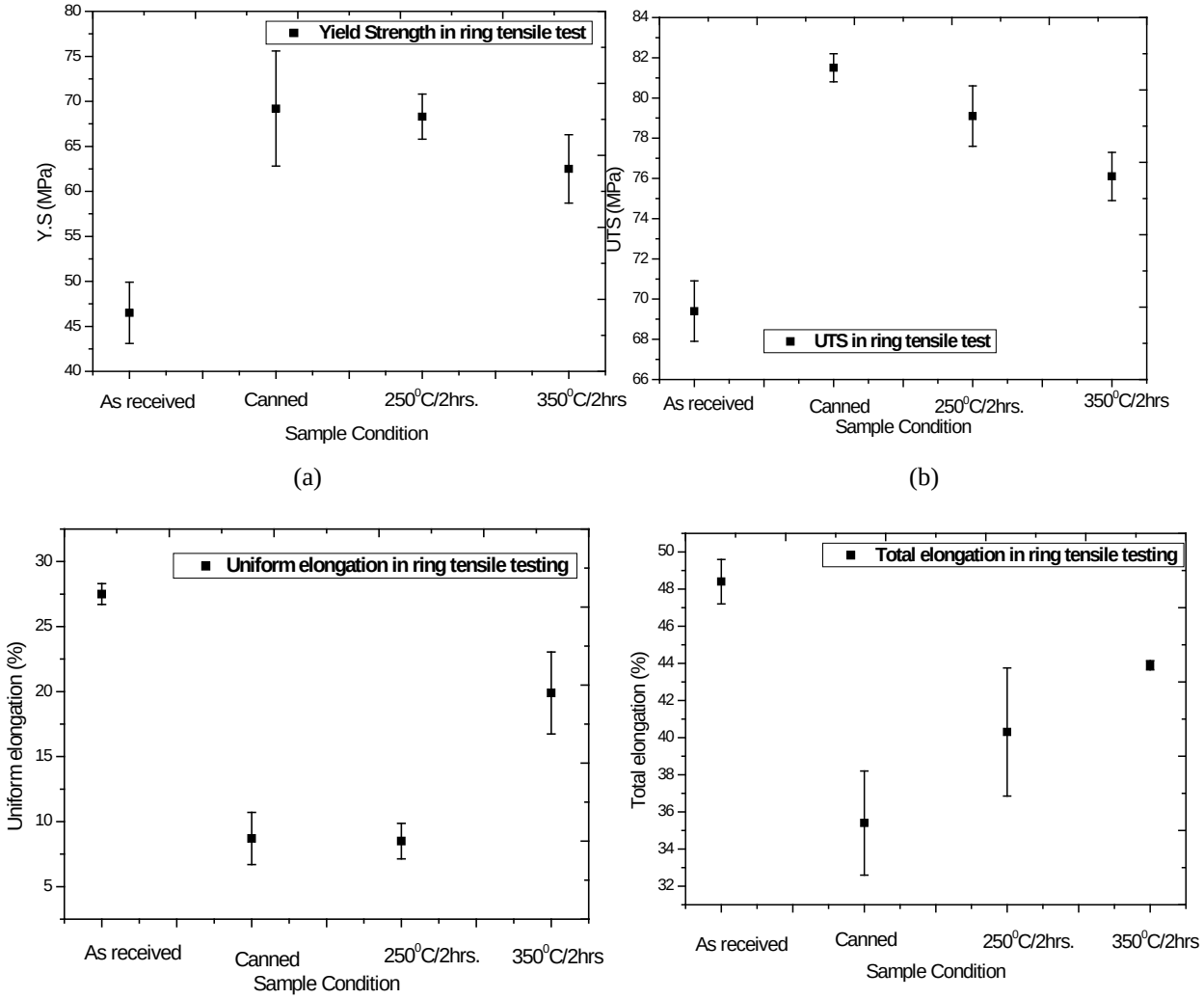


Fig. 7. a, b, c, d, show the plot of the average tensile properties Y.S, UTS, Uniform Elongation (%), Total Elongation (%) in ring tensile testing obtained for all the samples after different thermo-mechanical treatment of 1S Aluminium which clearly indicate the effectiveness of the stress relieving operation.

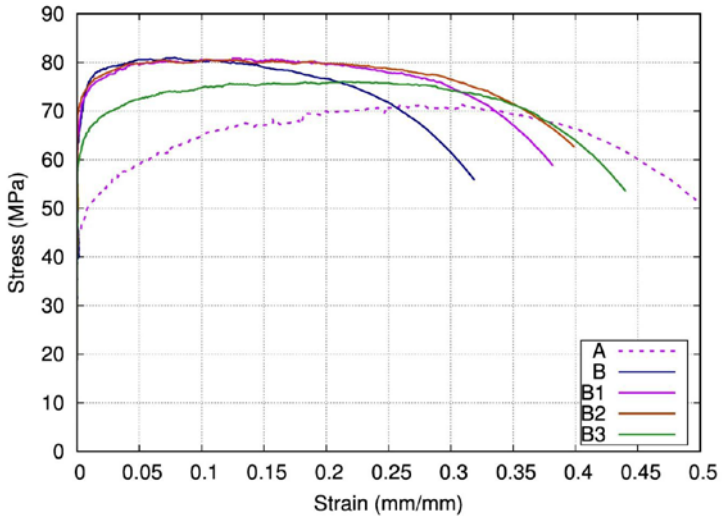


Figure 8. Typical engineering stress-strain plots obtained for specimens from different samples as given in Table 1 where A: as received sample, B: canned, B1 200ºC/2 hrs. heat treated, B2 250ºC/2hrs., B3:350ºC/2hrs.

## 5. Acknowledgements

The author is grateful to Dr (Mrs.) Priti Kotak Shah, Post Irradiation Division, BARC for carrying out ring tensile testing of the samples.

## 6. References

[1] N. Veeraraghavan, Research Reactor Dhruva , Proceedings of the international symposium on research reactor safety operations and modifications, Chalk River, ON (Canada); 23-27 Oct 1989, IAEA-SM-310/114, p1295-1309, https://inis.iaea.org/collection/NCLCollectionStore/_Public/22/047/22047730.pdf
[2] A. Leenaers, S. Van den Berghe, Microstructure of 50 year old SCK CEN BR1 research reactor fuel, RERTR-2007, the 29th international meeting on Reduced Enrichment for Research and Test Reactors, September 23-27, 2007, Prague, Czech Republic, https://www.rertr.anl.gov/RERTR29/PDF/11-5_Leenaers.pdf
[3] Rajiv Sikand, Arun M Kumar, Anil K Sachdev, Alan A Luo, Vipin Jain, Anil K Gupta, AM30 porthole die extrusions- A comparison with circular seamless extruded tubes, Journal of Material Processing Technology, 2009; 209: 6010–6020.
[4] M K Malik, Manufacture of aluminum alloy components for nuclear applications, Proceedings of National Symposium on Manufacture of Nuclear Components, April 7-8,1982, BARC, Mumbai, M12-1-M12-17.
[5] Gargi Choudhuri, R Pal, P Nanekar, D Mukherjee, Effect of Inhomogeneous Distribution of Alloying Elements on Integrity of Al-2.1 wt.% Mg Alloy Tubes and Welds, Journal of Materials and Applications, Journal of Materials and Applications, 2018; 7(2): 55-65.
[6] Akaret R, Extrusion welds-quality aspects are now center stage, Proceedings of the 5th International Aluminum Extrusion Technology Seminar Papers, Chicago, 1992. p.319-336.
[7] Plate M and Piwnik J, Theoretical and experimental analysis of seam weld formation in hot extrusion of aluminum alloys, Proceedings of 7th International Aluminum Extrusion Technology Seminar, Chicago, 2000, Vol.1, 205-211.
[8] Bourqui B, Huber A, Moulin C, A Bunetti Improved weld seam quality using 3D FEM simulation in correlation with practice, The first EAA extrusders division congress, Brescia Italy, 2002.
[9] Jo H H, Jeong C S, Lee S K, B M Kim, Determination of welding pressure in the non steady-state porthole die extrusion of improved Al7003 hollow section tubes, Journal of Material Processing Technology, 2003; 139 (1-3): 428-433.
[10] Fazzini P A B and Bellotti S, How to obtain quality profiles surfaces, Aluminio E Leghe 2008; 6: 81-85.
[11] Donati L and Tomesani L, The effect of die design on the production and seam weld quality of extruded aluminum profiles, Journal of Material Processing Technology, 2005 (164-165): 1025-1031.
[12] Ceretti E, Fratini L, Gagliardi F, C. Giardini, A new approach to study material bonding in extrusion porthole die, CIRP Annals Manufacturing Technology, 2009; 58(1): 259-262.
[13] Bingöl S, Keskin, M S and Bozaci A, Properties of seam welds produced with different extrusion parameters, Archives of Materials Science and Engineering, 2007; 28(6): 365- 368.
[14] Bingol S and Keskin M S, Effect of different extrusion temperature and speed on extrusion welds, Journal of Achievements in Materials and Manufacturing Engineering, 2007; 23(2): 39-42.
[15] Zhang C S, Zhao G Q, Chen Z R, H Chen, F J Kou, Effect of extrusion stem speed on extrusion process for a hollow aluminum profile, Materials Science and Engineering B - Advanced Functional Solid State Materials, 2012; 177: 1691-1697.
[16] Den Bakkera J A, Werkhoven R J, Sillekens W H, Katgerman L, The origin of weld seam defects related to metal flow in the hot extrusion alloys EN AW-6060 and EN AW-6082, Journal of Material Processing Technology, 2014; 214: 2349–2358.
[17] Valberg H, Loeken T, Hval M, Nyhus B, Thaulow C, The extrusion of hollow profiles with a gas pocket behind the bridge, International Journal of Materials and Product Technology, 1995;10(3-6): 222–267.
[18] Donati L, Tomesani L, The effect of die design on the production and seam weld quality of extruded aluminum profiles, Journal of Material Processing Technology, 2005; 164: 1025-1031.
[19] Mukherjee D, Non destructive characterization for quality control of nuclear fuels, Proceedings of the conference on indigenous nuclear fuel program in India - achievements, status and prospects "INFPIN-2019", 31 Jan - 2 Feb 2019, Mumbai (India).
[20] K Kapoor, D Lahiri, S V R RAO, T Sanyal and B P Kashyap, X-ray diffraction line profile analysis for defect study in Zr–2.5% Nb material, Bulletin of Materials Science, 2004; 27(1): 59–67.
[21] Gargi Choudhuri, Jagannath, M Kiran Kumar, V. Kain, D. Srivastava, S. Basu, B.K. Shah, N. Saibaba, G.K. Dey, Influence of Fe content on corrosion and hydrogen pick up behaviour of Zr–2.5Nb pressure tube material, Journal of Nuclear Materials, 2013; 441:178–189.

[22] E J Mittemeijer, P. Scardi (Eds.), Diffraction Analysis of the Microstructure of Materials, Springer Series in Materials Science, 2004; 68.
[23] K Yvell, T M Grehk, P Hedström, A Borgenstam, G. Engberg, EBSD analysis of surface and bulk microstructure evolution during interrupted tensile testing of a Fe-19Cr-12Ni alloy, Materials Characterization, 2018; 141: 8–18.
[24] F J Humphreys, Quantitative metallography by electron backscattered diffraction Journal of Microscopy, 1999;195: 170-185.
[25] H Jazaeri, F J Humphreys, Quantifying recrystallization by electron backscatter diffraction, Journal of Microscopy, 2004; 213(3): 241–246.
[26] H D Merchant, G S Murty, S N Bahadur, L.T. Dwivedi, Y. Mehrotra, Hardness-temperature relationships: in metals, Journal of Materials Science, 1973; 8: 437- 442.
[27] Preeti Kotak Shah, Ring tensile properties of Aluminium clad. Technical report BARC/PIED/2020/TR09, 2020.